Pharm Res (2014) 31:1469–1476
DOI 10.1007/s11095-013-1008-5

RESEARCH PAPER

Synthesis and Evaluation of a Targeted Nanoglobular Dual-Modal Imaging Agent for MR Imaging and Image-Guided Surgery of Prostate Cancer

Mingqian Tan • Zhen Ye • Daniel Lindner • Susann M. Brady-Kalnay • Zheng-Rong Lu

Received: 8 December 2012 / Accepted: 7 February 2013 / Published online: 8 March 2013

ABSTRACT

Purpose To synthesize and evaluate a peptide targeted nanoglobular dual modal imaging agent specific to a cancer biomarker in tumor stroma for MRI and fluorescence visualization of prostate tumor in image-guided surgery.

Methods A peptide (CGLIIQKNEC, CLT1) targeted generation 2 nanoglobular (polylysine dendrimer with a silsesquioxane core) dual modal imaging agent, CLT1-G2-(Gd-DOTA-MA)-Cy5, was synthesized by stepwise conjugation of Gd-DOTA-MA, Cy5 and peptide to the dendrimer. Contrast enhanced MR imaging of the targeted dual imaging agent was evaluated on a Bruker 7T animal scanner with male athymic nude mice bearing orthotopic PC3-GFP prostate tumor. Fluorescence tumor imaging of the agent was carried out on a Maestro fluorescence imaging system.

Results The targeted agent CLT1-G2-(Gd-DOTA-MA)-Cy5 produced greater contrast enhancement in the tumor tissue than the control agent KAREC-G2-(Gd-DOTA-MA)-Cy5 at a dose of 30 μmol-Gd/kg in the MR images of the tumor bearing mice. Signal-to-noise ratio (SNR) of CLT1-G2-(Gd-DOTA-MA)-Cy5 in the tumor tissue was approximately 2 fold of that of the control agent in the first 15 min post-injection. The targeted agent also resulted in bright fluorescence signals in the tumor tissue.

Conclusion The CLT1 peptide targeted nanoglobular dual-imaging agent CLT1-G2-(Gd-DOTA-MA)-Cy5 has a potential for MRI and fluorescence visualization of prostate tumor.

KEY WORDS contrast agent · dual modal imaging agent · fluorescence imaging · image guided surgery · MRI

INTRODUCTION

Accurate detection and localization of malignant tumors is crucial to improve effectiveness of cancer treatments and interventions. Various imaging modalities, including X-ray computed tomography (CT), magnetic resonance imaging (MRI), positron emission tomography (PET) and single photon emission computed tomography (SPECT), have been broadly used in the clinical practice for cancer detection and diagnosis. Recently, intraoperative optical imaging has been developed to assist tumor localization and to guide surgical tumor resection (1–3). The combination of non-invasive anatomic diagnostic imaging and intraoperative optical imaging would be valuable for accurate tumor localization and image-guided surgery. MRI is a non-ionizing imaging modality and provides three-dimensional high-resolution images of soft tissues. Contrast enhanced MRI with a tumor specific contrast agent can non-invasively detect malignant tumors before surgery interventions. Fluorescence imaging has high sensitivity for detecting cancer biomarkers and can accurately delineate tumor boundary to guide tumor resection based on the cancer related biomarkers.(4–6) The design and development of a

M. Tan • Z. Ye • Z.-R. Lu (✉)
Department of Biomedical Engineering
Case Western Reserve University
Wickenden Building, Room 427, 10900 Euclid Avenue
Cleveland, Ohio 44106-7207, USA
e-mail: zxl125@case.edu

M. Tan
Laboratory of Biomedical Material Engineering
Dalian Institute of Chemical Physics, Chinese Academy of Sciences
Dalian 116023 People's Republic of China

D. Lindner
Department of Translational Hematology & Oncology Research
Cleveland Clinic, Cleveland, Ohio 44195, USA

S. M. Brady-Kalnay
Department of Molecular Biology and Microbiology
School of Medicine, Case Western Reserve University
Cleveland, Ohio, USA

tumor specific molecular imaging agent containing both an MRI contrast agent and a fluorescence dye will enable the combination of two imaging modalities for tumor detection localization by MRI and image-guided surgery by fluorescence imaging.

Various dual imaging agents containing both MRI contrast agent and fluorescence dye have been reported in the literature.(7–10) Mishra *et al.* synthesized a class of bifunctional probes based on DO3A-ethylthioureido-fluorescein conjugates ([4,7-bis-carboxymethyl-10-(2-(fluorescein-thioureido)ethyl)-1,4,7,10-tetraaza-cyclododec-1-yl]-acetic acid) for both MR and optical imaging.(11) Mulder *et al.* reported RGD targeted quantum dots coated with Gd-DTPA-bisamide and pegylated lipids.(12) Pfaff *et al.* developed core-shell magnetic and fluorescence nanospheres by grafting a glycocopolymer consisting of 6-O-methacryloylgalactopyranose (MAGal) and 4-(pyrenyl) butylmethacrylate (PyMA) onto iron oxide nanoparticles.(13) Some of these agents have shown very high relaxivities and are effective for both MRI and fluorescence imaging. However, the dual imaging agents suitable for clinical development should possess good tumor targeting ability as well as high safety profiles. Rational design of targeted dual-imaging agents for MRI and fluorescence imaging with good safety profiles is important for detection and localization of malignant tumor and image-guided surgery.

We have recently reported that CLT1 peptide (CGLIIQKNEC) targeted nanoglobular Gd-DOTA monoamide conjugates are effective for MR cancer molecular imaging of a cancer related biomarker in tumor stroma. (14, 15) CLT1 is a cyclic peptide and specifically binds to the fibrin-fibronectin complexes in the extracellular matrix of different tumors with little binding to normal tissues.(16) Nanoglobules, lysine dendrimers with a silsesquioxane core, are a unique class of dendrimers with high surface functionality, nanoscopic dimension and well-defined structure.(17) The high surface functionality allows the conjugation of the peptide, a relatively large number of Gd-DOTA monoamide and other imaging probes.(15) The peptide targeted generation 2 (G2) nanoglobular conjugate produced strong enhancement in tumor tissue, including orthotopic prostate tumor, at a reduced dose (0.03 mmol-Gd/kg).(15, 18) Its relatively small size (ca. 5.6 nm) allows rapid excretion of free conjugate via renal filtration, resulting in minimal tissue Gd retention.

Herein, we report the synthesis and evaluation of a CLT1 peptide targeted G2 nanoglobular Gd-DOTA monoamide and cyanine 5 conjugate CLT1-G2-(Gd-DOTA-MA)-Cy5 as a targeted dual imaging agent. The targeted nanoglobular dual imaging agent was synthesized by stepwise conjugation of Gd-DOTA monoamide, Cy5 and peptide. Tumor MRI and fluorescence imaging of the dual-imaging agent was investigated at a dose of 30 μmol-Gd/kg in athymic mice bearing orthotopic PC3-GFP prostate tumor.

MATERIALS AND METHODS

2-(1*H*-Benzotriazol-1-yl)-1,1,3,3-tetramethyluronium hexafluorophosphate (HBTU), benzotriazol-1-yl-oxytripyrrolidinophosphonium hexafluorophosphate (PyBOP), and 1-hydroxybenzotriazole hydrate (HOBt) were purchased from Nova Biochem (Darmstadt, Germany). 1,4,7,10-Tetraazacyclododecane-1,4,7-tris-*tert*-butyl acetate-10-acetic acid [DOTA-tris(t-Bu)] was purchased from Macrocyclics (Dallas, TX). 3-[(2-Azido-ethylenoxy)-hepta(2-ethylenoxy)]-propionic N-hydroxysuccinimide ester (Azido-PEG-NHS) and 3-propargyloxy-propionic N-hydroxysuccinimide ester (propargyl-PEG-NHS) were purchased from Quanta BioDesign (Powell, OH). N^{ε}-Boc-*L*-lysine was purchased from EMD Chemicals Inc. (Gibbstown, New Jersey). Fluorophore cyanine 5 (Cy5) mono-reactive NHS ester was purchased from GE Healthcare (Buckinghamshire, UK). Anhydrous diisopropylethylamine (DIPEA), dimethyl sulfoxide (DMSO) and N,N-dimethylformamide (DMF) were purchased from Alfa Aesar (Ward Hill, MA). Trifluoroacetic acid (TFA) was purchased from ACROS Organics (Morris Plains, NJ). Peptide CLT1 and non-specific control peptide (KAREC) were synthesized using standard solid phase peptide chemistry from Fmoc-protected amino acids on a 2-chlorotrityl chloride resin. PC3 human prostate adenocarcinoma cells were obtained from American Type Culture Collection (ATCC, Manassas, VA). All reagents were used without further purification unless otherwise stated.

Synthesis of N^{α}-(3-[(2-azido-ethylenoxy)-hepta(2-ethylenoxy)]-propionyl)-N^{ε}-(t-butoxycarbonyl)lysine (Compound 1)

N^{ε}-Boc-*L*-lysine (45.8 mg, 0.186 mmol), azido-PEG NHS (100 mg, 0.177 mmol), and an excess of DIPEA were dissolved in a mixture of DMF and dichloromethane (3 mL, volume/-volume = 1:1) and stirred at room temperature for 24 h. The solvent was evaporated under vacuum and the residue was purified by recrystallization. Yield of compound 1 was 123 mg, 96%. MALDI-TOF (m/z, $[M+Na]^+$): 718.27 (measured), 718.79 [calculated for compound 1, $C_{30}H_{57}N_5O_{13}$]. ^{1}H NMR (300 MHz, $CDCl_3$, ppm): 1.26 (t, 2H), 1.43 (m, 13H), 2.53 (t, 2H), 2.68(t, 2H), 3.09(t, 2H), 3.39(t, 2H), 3.64(m, 2H), 3,66 (t, 28H), 4.45 (m, 1H).

Synthesis of G2 Nanoglobule-(lysine-PEG-N_3)$_3$ Conjugate (Compound 2)

Generation 2 (G2) nanoglobule, polylysine dendrimers with an octa(3-aminopropyl)silsesquioxane core, were synthesized as previously described.(17) G2 nanoglobule (100 mg, 13.2 μmol), compound 1 (45 mg, 66 μmol), HBTU (25 mg, 66 μmol), HOBt (8.9 mg, 66 μmol) and 200 μL of DIPEA were dissolved in 2 mL DMF and stirred at room temperature

overnight. The residue was treated with ice-cold diethyl ether to give a colorless solid. The precipitate was dissolved in pure water and further purified by ultrafiltration using Millipore's Amicon® Ultra-15 centrifugal filters (3 kDa molecular weight cutoff). Yield of G2 nanoglobule-(lysine-PEG-N_3)$_3$ conjugate was 136 mg, 83.9%. MALDI-TOF (m/z, $[M+H]^+$): 6,034 (measured), 5,997 [calculated for G2 nanoglobule-(lysine-PEG-N_3)$_3$].

Synthesis of G2 Nanoglobule-(Gd-DOTA)$_{20}$-(lysine-PEG-N_3)$_3$ Conjugate. (Compound 3)

G2 nanoglobule-(lysine-PEG-N_3)$_3$ conjugate (136 mg, 13 μmol), DOTA-tris(*t*-Bu) (416 mg, 728 μmol), HBTU (276 mg, 728 μmol), HOBt (98 mg, 728 μmol) and DIPEA (0.5 mL) were dissolved in DMF (3 mL) and stirred at room temperature for 60 h. After reaction, the product was added to anhydrous diethyl ether. The oil-like precipitate was washed several times with diethyl ether and the protecting groups were removed by dissolving the precipitate in a mixture of TFA and dichloromethane (5 mL, volume/volume = 1:1) for 4 h while stirring at room temperature. The residue was treated with ice-cold diethyl ether to give a colorless solid. The precipitate was dissolved in pure water and further purified by ultrafiltration using Millipore's Amicon® Ultra-15 centrifugal filters (3 kDa molecular weight cutoff). A Kaiser test was then performed to confirm the presence of primary amine groups. Yield of G2 nanoglobule-(DOTA)$_{20}$-(lysine-PEG-N_3)$_3$ conjugate was 152 mg, 70%. MALDI-TOF (m/z, $[M+H]^+$): 13,968 (measured), 14,017 [calculated for G2 nanoglobule-(DOTA)$_{20}$-(lysine-PEG-N_3)$_3$].

G2 nanoglobule-(DOTA)$_{20}$-(lysine-PEG-N_3)$_3$ conjugate (152 mg, 10.8 μmol) in 4.0 mL deionized water was mixed with Gd(OAc)$_3$ (765 mg, 1.66 mmol) and stirred at room temperature for 4 days. The excess free Gd^{3+} ions were removed from the solution by adding EDTA and eluting through a PD-10 desalting column with deionized water. The product G2 nanoglobule-(Gd-DOTA)$_{20}$-(lysine-PEG-N_3)$_3$ conjugate was further purified by dialysis with a membrane with a molecule weight cutoff of 1,000 Da at room temperature. Yield of G2 nanoglobule-(Gd-DOTA)$_{20}$-(lysine-PEG-N_3)$_3$ was 31 mg, 64%. A Kaiser test was then performed to confirm the presence of primary amine groups on the compound 3.

Synthesis of G2 Nanoglobule-(Gd-DOTA)$_{20}$-(lysine-PEG-N_3)$_3$-Cy5 Conjugate. (Compound 4)

G2 nanoglobule-(Gd-DOTA)$_{20}$-(lysine-PEG-N_3)$_3$ conjugate (36 mg, 2 μmol), Cy5 mono-NHS ester (5 mg, 7.2 μmol), PyBOP (11 mg, 21.6 μmol), HOBt (3 mg, 21.6 μmol) and DIPEA (20 μL) were dissolved in DMSO (1 mL) and stirred at room temperature for 24 h. After reaction, the product was added to water and the hydrophobic impurities were removed by filtration. The filtrate was purified by ultrafiltration using Millipore's Amicon® Ultra-15 centrifugal filters (3 kDa molecular weight cutoff). Yield of G2 nanoglobule-(Gd-DOTA)$_{20}$-(lysine-PEG-N_3)$_3$-Cy5 conjugate was 34 mg, 87%. The number of Cy5 attached onto G2 nanoglobular conjugate was approximately one on average as determined by UV spectroscopy.

Synthesis of CLT1-G2-(Gd-DOTA-MA)-Cy5 (Compound 5)

CLT1 peptide was conjugated to G2 nanoglobule-(Gd-DOTA)$_{20}$-(lysine-PEG-N_3)$_3$-Cy5 conjugate via "click chemistry" between the reactive propargyl group of the peptide conjugate (15) and azido group of the nanoglobule-(Gd-DOTA)$_{20}$-(lysine-PEG-N_3)$_3$-Cy5 conjugate. G2 nanoglobule-(Gd-DOTA)$_{20}$-(lysine-PEG-N_3)$_3$-Cy5 conjugate (54 mg, 2.0 μmol) and ascorbic acid (3.6 mg, 2.0 μmol) were dissolved in 2 mL water, followed by the addition of copper(II) sulfate pentahydrate (0.5 mg, 2.0 μmol). Then peptide-PEG-propargyl conjugate (23 mg, 16 μmol) in 2 mL of DMSO/*tert*-butyl alcohol (1:1, v/v) was added to above solution and the reaction was stirred vigorously for 40 h at room temperature. The precipitate was removed by filtration. The product was purified by ultrafiltration and dialysis (molecule weight cutoff = 1,000 Da) at room temperature to remove any small molecular impurities. Yield of the peptide dual imaging agent CLT1-G2-(Gd-DOTA-MA)-Cy5 was 20 mg, 32.9%. The Gd(III) content measured by inductively coupled plasma optical emission spectroscopy (ICP-OES Optima 3100XL, Perkin-Elmer) was 10.37% wt/wt. The Cy5 content in the conjugate was determined by UV spectrophotometry. There were three peptides in each conjugate on average as estimated from sulfur content determined by ICP-OES.

Synthesis of Control Agent KAREC-G2-(Gd-DOTA-MA)-Cy5

The control peptide KAREC modified G2 nanoglobular agent KAREC-G2-(Gd-DOTA-MA)-Cy5 was similarly prepared as described in "Synthesis of CLT1-G2-(Gd-DOTA-MA)-Cy5 (Compound 5)" by reacting KAREC-PEG-propargyl conjugate (2.2 mg, 2.4 μmol) with compound 4 (12 mg, 0.4 μmol). The yield of the final product KAREC-G2-(Gd-DOTA-MA)-Cy5 was12.84 mg, 99%. The Gd(III) content measured by ICP-OES was 10.50% wt/wt. There were three peptides in each conjugate on average as estimated from sulfur content determined by ICP-OES.

Orthotopic PC3 Prostate Tumor Model

PC3 human prostate adenocarcinoma cells were cultured in Roswell Park Memorial Institute (RPMI) medium supplemented with 5% fetal bovine serum and penicillin/streptomycin/fungizone. The cells were infected with lentivirus to express green fluorescent protein (GFP) at least 48 h prior to harvesting. PC3-GFP Cells were harvested for prostate implantation by trypsinization and concentrated in RPMI medium. The cell suspension was loaded into a syringe fitted with a 27 gauge needle. NIH athymic nude male mice, age 4–5 weeks, were maintained at the Athymic Animal Core Facility at Case Western Reserve University according to institutional guidelines. All animal protocols were approved by the Institutional Animal Care and Use Committee (IACUC). Mice were anesthetized by intraperitoneal injection of Avertin. A small midline incision was made through the skin and underlying musculature in the abdominal region overlying the bladder. The bladder was reflected through the incision to expose the prostate gland. Approximately 20 μl concentrated PC3-GFP cells were injected into the prostate, and the incision was closed with staples. The staples were removed 10 days later. The growth of PC3-GFP prostate tumor was monitored using the Maestro FLEX *In Vivo* Imaging System after cell injection.

Contrast Enhanced MR Tumor Imaging

After the tumor size reached about 0.3–0.5 cm in diameter, MRI study was carried out on a Bruker Biospec 7T MRI scanner (Bruker Corp., Billerica, MA, USA) with a volume radio frequency (RF) coil. The mice were randomly divided into groups ($N=4$) for MR molecular imaging study. Animals were anesthetized with 2% isoflurane with supplemented O_2 continuously during the whole imaging process via a nose cone. Electrodes were attached to front paws and right leg for ECG monitoring vital signs through an MR-compatible small animal gating and monitoring system (SA Instruments, Stony Brook, NY). The anesthetized animals' body temperature was maintained at 35 ± 1°C by blowing hot air into the magnet through a feedback control system. The heat flow and the anesthesia level were manually adjusted to maintain the heart rate close to that under conscious condition. A 30-gauge needle was inserted into the tail vein and connected to a syringe through a flexible plastic tubing (Tygon®, Saint-Gobain PPL Corp. Akron, OH) for contrast agent administration. The dual-imaging agents were administered via the tail vein at a dose of 30 μmol-Gd/kg body weight.

The mice were scanned before the injection and at 1, 5, 10, 15, 20, 25, 30, 35, and 40 min post-injection using Bruker *gradient-echo* T_1-weighted MRI sequence (TR/TE = 151.2/1.9 ms, number of averages = 1, flip angle = 30°, total acquisition time = 19 s, slice thickness = 1.2 mm, field of view = 3.0 cm, matrix = 256×256, slice number = 12). Image analysis was performed using Bruker ParaVision 4.0 imaging software. Regions of interest were drawn over the whole tumor in the 2D images. Signal intensity (S) was measured at each time point and averaged from the tumors of the mice ($N=4$). The signal to noise ratio (SNR) was calculated using the following equation: $SNR = (S - S_0)/\sigma_n$; where S (post-injection) and S_0 (pre-injection) denote the signal within the regions of interest (ROIs) and σ_n is the standard deviation of noise estimated from the background air. Statistical analysis was performed using a two-way ANOVA with Bonferroni's, assuming statistical significance at $p<0.05$.

Tumor Fluorescence Imaging

Fluorescence imaging of PC3-GFP prostate tumor was performed on a Maestro FLEX *In Vivo* Imaging System using the appropriate filters for GFP (excitation: 444–490 nm; emission: 515 nm long-pass filter; acquisition settings: 500–720 in 10 nm steps) and Cy5 (excitation: 576–621 nm; emission: 635 nm long-pass filter; acquisition settings: 630–800 in 10 nm steps). Acquisition settings were 10 ms for GFP and 61 ms for the Cy5 conjugates. The mice were sacrificed 2 h after the intravenous injection of CLT1-G2-(Gd-DOTA-MA)-Cy5 and KAREC-G2-(Gd-DOTA-MA)-Cy5 (10 nmol Cy5 per mouse). Both GFP and Cy5 fluorescence images of the tumor and various organs were then acquired. The fluorescent signal was spectrally separated from the multispectral fluorescence images with Maestro software (Cambridge Research & Instrumentation, Inc, Woburn, MA) to subtract the background autofluorescence.

RESULTS

Synthesis of the Dual Modal Imaging Agent

The synthesis of the peptide targeted dual imaging agent CLT1-G2-(Gd-DOTA-MA)-Cy5 and the control agent KAREC-G2-(Gd-DOTA-MA)-Cy5 is shown in Scheme 1. The azido-PEG and lysine conjugate (compound 1) was synthesized as a bifunctional linker for the conjugation of the targeting peptide and cyanine 5. G2 nanoglobule had 32 surface amino groups for conjugation of the targeting agent and imaging agents. In order to maximize conjugation degree of Gd-DOTA-MA to the dendrimer and minimize possible fluorescence quench of Cy by the Gd(III) chelates, Cy5 was conjugated to the ε-amino group of lysine in the compound 1 after conjugation of Gd-DOTA-MA. Approximately 3 linker molecules and 20 DOTA-MA chelates on average were conjugated to each dendrimer. Approximately 63% of the amino groups were conjugated with DOTA-MA even in the

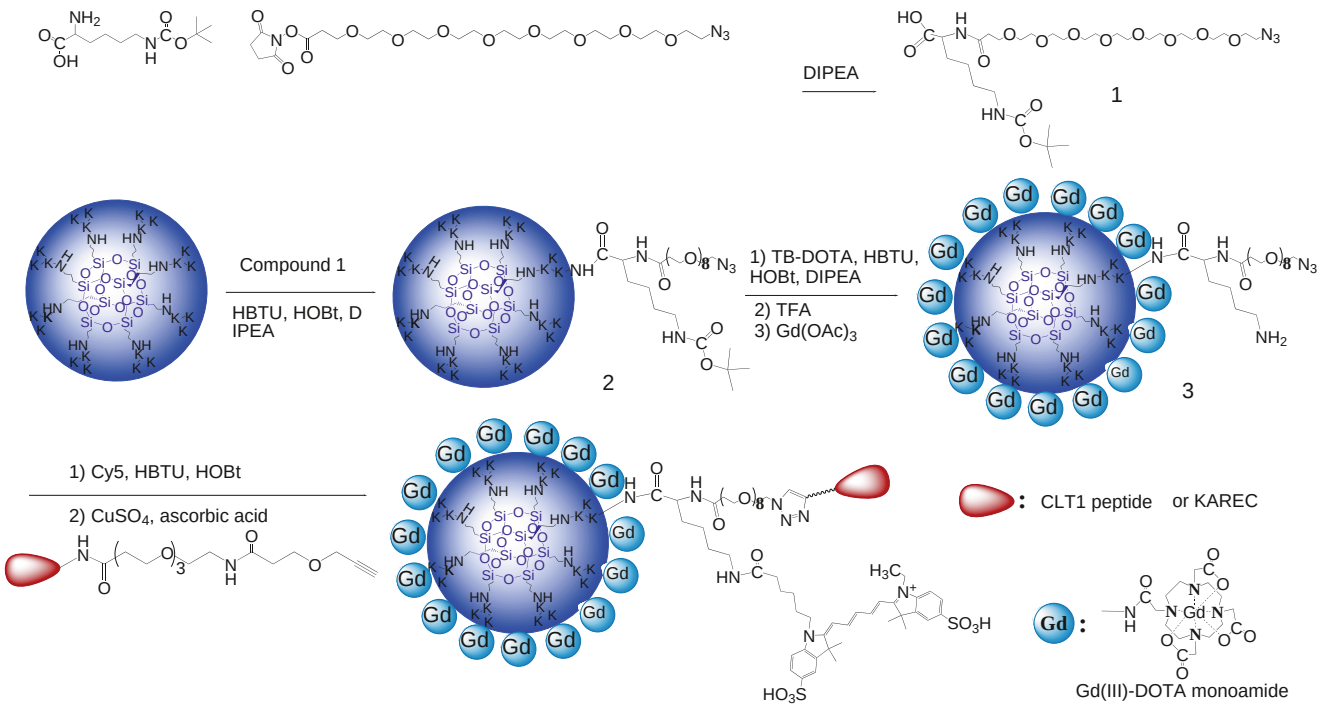

Scheme 1 Synthesis scheme of the nanoglobular dual imaging agents CLT1-G2-(Gd-DOTA-MA)-Cy5 and KAREC-G2-(Gd-DOTA-MA)-Cy5.

presence of an excess of the ligands. The presence of free amino group in the nanoglobular conjugate was confirmed by Kaiser test. Gadolinium(III) was then reacted with nanoglobular ligands at room temperature for 4 days to assure complete complexation of the ligand. Approximately one Cy5 molecule was conjugated to the ε-amino group of the lysine residues on the linker after the deprotection. Finally, three peptide molecules (CLT1 or KAREC) was conjugated to the dendrimer via click chemistry. Less Cy5 molecule was conjugated to the dendrimer than the peptides, possibly because of the steric effect of the PEG and dendrimer in the conjugation reaction with Cy5 active ester.

The physicochemical parameters of the dual-imaging agents are listed in Table I. The r_1 and r_2 relaxivities of the targeted agent were 13.4 and 14.6 $mM^{-1}s^{-1}$ per Gd(III) chelate at 1.5 T, and 12.2 and 13.9 $mM^{-1}s^{-1}$ per Gd(III) chelate for the control agent. Both peptide targeted dual-imaging agents had similar physicochemical properties. KAREC-G2-(Gd-DOTA-MA)-Cy5 was an appropriate control for CLT1-G2-(Gd-DOTA-MA)-Cy5 for tumor imaging. Both CLT1-G2-(Gd-DOTA-MA)-Cy5 and KAREC-G2-(Gd-DOTA-MA)-Cy5 had the same fluorescence spectra of cyanine 5.

Contrast-Enhanced MR Tumor Imaging

The effectiveness of the targeted dual imaging agent CLT1-G2-(Gd-DOTA-MA)-Cy5 in contrast enhanced MR tumor imaging was demonstrated in male nude mice bearing orthotopic prostate tumor. Figure 1 shows the T_1-weighted 2D axial MR images of the orthotopic prostate tumor contrast enhanced with CLT1-G2-(Gd-DOTA-MA)-Cy5 and KAREC-G2-(Gd-DOTA-MA)-Cy5. The targeted agent CLT1-G2-(Gd-DOTA-MA)-Cy5 resulted in strong enhancement in the tumor tissue, particularly in the tumor periphery at 5 min post-injection. The enhancement gradually decreased over time, but substantial enhancement was still visible at 40 min post-injection. KAREC-G2-(Gd-DOTA-MA)-Cy5 also produced visible enhancement in tumor periphery due to the passive EPR effect. However, the tumor enhancement with KAREC-G2-(Gd-DOTA-MA)-Cy5 was weaker than that with CLT1-G2-(Gd-DOTA-MA)-Cy5. The tumor

Table I Physicochemical Properties of the Nanoglobular MRI Contrast Agents

Imaging agents	Gd content (wt.%)	No. of Gd-DOTA-monoamide chelates	No. of surface Peptide	No. of surface Cy5	Molecular weight (KDa)	r_1/r_2 [$mM^{-1}s^{-1}$ per Gd] at 1.5 T
Targeted Control	10.37	~20/32	~ 3	~ 1	30.3	13.4/14.6
	10.50	~20/32	~ 3	~ 1	29.9	12.2/13.9

Targeted: peptide CLT1-G2-(Gd-DOTA-MA)-Cy5; Control: KAREC-G2-(Gd-DOTA-MA)-Cy5

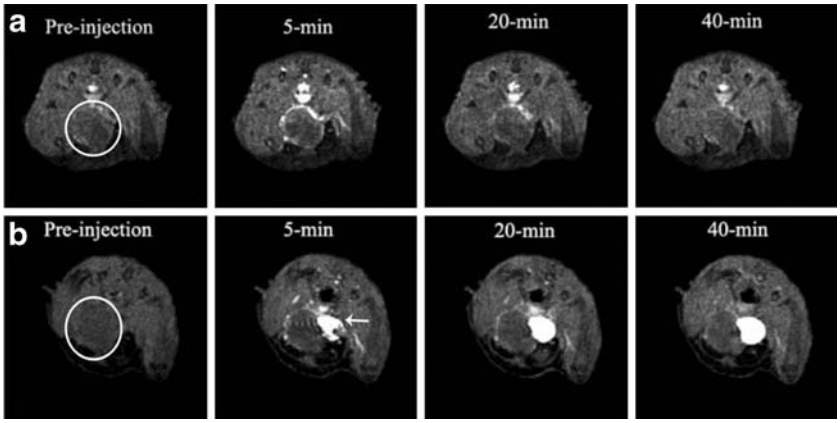

Fig. 1 Representative T_1-weighted 2D axial MR images of mouse orthotopic prostate tumor before and after intravenous injection of CLT1-G2-(Gd-DOTA-MA)-Cy5 (**a**) and KAREC-G2-DOTA-Gd (**b**) at 30 μmol-Gd/kg body weight. ($N = 4$) The solid arrow points to the urinary bladder. The circle highlights the tumor region.

size was approximately 5 mm in diameter as estimated from the MR images with Bruker ParaVision 4.0 imaging software.

Quantitative analysis of signal intensity in the tumor tissue revealed that CLT1-G2-(Gd-DOTA-MA)-Cy5 resulted in 100% more signal-to-noise ratio (SNR) than the control KAREC-G2-(Gd-DOTA-MA)-Cy5 in the first 15 min post-injection, Fig. 2. CLT1-G2-(Gd-DOTA-MA)-Cy5 produced significantly greater SNR within the tumor than the control agent for up to 30 min post-injection ($p < 0.05$). At least 50% more SNR was still observed in the tumor with CLT1-G2-(Gd-DOTA-MA)-Cy5 than KAREC-G2-(Gd-DOTA-MA)-Cy5 at the end of the experiment (40 min post injection). The difference in SNR of CLT1-G2-(Gd-DOTA-MA)-Cy5 and KAREC-G2-(Gd-DOTA-MA)-Cy5 gradually decreased over time possibly due to the *in vivo* degradation of peptide for the targeted agent. CLT1-G2-(Gd-DOTA-MA)-Cy5 exhibited significantly higher tumor binding efficiency than the control agent in the first 30 min ($p < 0.05$). With the increase of the time, the peptide of CLT1-G2-(Gd-DOTA-MA)-Cy5 might be degraded *in vivo* by the enzymes in the tissue, while the non-specific accumulation of KAREC-G2-(Gd-DOTA-MA)-Cy5 did not change significantly during the period of the experiment. As a result, the difference in SNR seems to decrease with time.

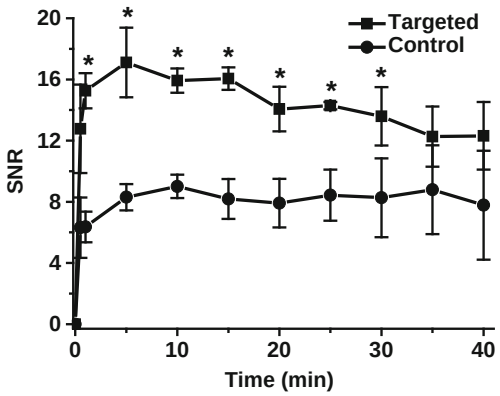

Fig. 2 Signal-to-noise (SNR) in the tumor with CLT1-G2-(Gd-DOTA-MA)-Cy5 (Targeted) and KAREC-G2-(Gd-DOTA-MA)-Cy5 (Control) administrated at 30 μmol-Gd/kg in the orthotopic prostate tumor bearing mice ($N = 4$). * $p < 0.05$.

Fluorescent Imaging of Prostate Tumor

Figure 3 shows the GFP and Cy5 fluorescence images of the tumor and major organs acquired 2 h after the injection of CLT1-G2-(Gd-DOTA-MA)-Cy5. The PC3 tumor tissue was labeled with strong green fluorescence from GFP. Substantial fluorescence of Cy5 from CLT1-G2-(Gd-DOTA-MA)-Cy5 was observed in the whole tumor tissue, while little red fluorescence was detected in other organs except the lung. The targeted agent CLT1-G2-(Gd-DOTA-MA)-Cy5 exhibited substantial specific binding in the tumor tissue.

DISCUSSION

The concept of using multiple modalities in conjunction with cancer treatment has drawn great attention to utilize the complementary abilities of different imaging modalities to achieve better treatment or intervention under imaging guidance.(9, 19, 20) In the study, we have synthesized and evaluated a peptide targeted nanoglobular dual modal imaging agent for cancer molecular imaging with MRI and fluorescence imaging. The nanoglobules are a class of highly branched lysine dendrimers with high surface functionality and precisely controlled sizes, suitable for conjugation of

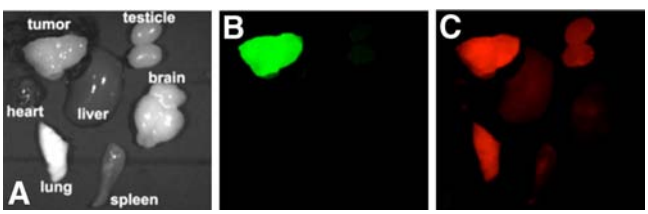

Fig. 3 Bright field image (**a**), GFP (**b**) and CY5 (**c**) fluorescence images of tumor and other major organs from mice bearing orthotopic GFP-expressed PC3 prostate xenograft tumors 2 h after intravenous injection of CLT1-G2-(Gd-DOTA-MA)-Cy5 at a Cy5 dose of 10 nmol.

multiple imaging agents and biologically active agents.(15, 17, 21, 22) The nanoglobules have more surface functional groups than other dendrimers, e.g., PAMAM dendrimers, of the same generation. High surface functional groups allow the conjugation of the targeting agent, fluorescence dye and a relatively large number of Gd-DOTA-MA chelates. CLT1 peptide was developed for targeting the fibrin-fibronectin complexes in tumor stroma in various cancers.(16) It has been reported that fibronectin is highly expressed in prostate cancer, much higher than in benign tumors and normal prostate tissue.(23) Our previous study showed that the peptide could specifically bind to the orthotopic prostate tumor tissue.(18) A competitive study also showed that the presence of an excess of free peptide could reduce the binding of a CLT1 targeted imaging agent in tumor tissue.(24) The CLT1 peptide could be an effective targeting agent for the development of targeted dual modal imaging agent for cancer molecular imaging with MRI and fluorescence imaging. As compared with monoclonal antibodies, the use of small molecular CLT1 peptide may reduce the immune reaction caused by the exogenous antibodies and minimize the overall size of the targeted dual imaging agent to facilitate complete elimination of the unbound agent from the body via renal filtration. Complete excretion of Gd(III) based contrast agents is necessitated for their safety in clinical development.

The targeted nanoglobular dual-imaging agent CLT1-G2-(Gd-DOTA-MA)-Cy5 had a high T_1 relaxivity and produced greater enhancement in the periphery of orthotopic prostate cancer than KAREC-Cy5-G2-DOTA-Gd. Since the r_1 relaxivities of both agents are similar, the strong enhancement in tumor with the CLT1 targeted agent should be attributed to the specific binding of the agent in the tumor. The targeted agent also provided better delineation of the boundary of the tumor tissue. MRI provides high-resolution 3D anatomic images of soft tissues. Better tumor delineation would allow more accurate construction of three-dimensional tumor volumes, which could be useful for better planning surgical procedures.

Fluorescence imaging of the dissected tumor tissues showed the overlap of the red fluorescence of Cy5 from the targeted conjugate with GFP from the tumor. The binding of the peptide to the fibrin-fibronectin complexes in tumor stroma allowed tumor visualization with fluorescence imaging 2 h after the injection of the targeted dual imaging agent. The targeted agent also showed significant non-specific binding in the lung. However, such non-specific binding was not observed with CLT1-Cy5 conjugate in our previous study.(15) The non-specific binding of the targeted nanoglobular dual imaging agent could be caused by the relatively large size of the agent and free amines due to incomplete surface conjugation. It was previously reported that positive charged nanosized materials had a high tendency for non-specific accumulation in the lung.(25–27) Further structure optimization of the targeted dual imaging agents is necessary to minimize non-specific tissue accumulation. We have shown in the a recent study that a CLT1 peptide targeted Gd-DOTA-MA conjugate of a low molecular weight was also effective to produce significant tumor enhancement in the orthotopic prostate cancer model at the same reduced dose. The design of a small molecular CTL1 targeted dual imaging agent may be a possible approach to minimize non-specific tissue accumulation of the targeted dual imaging agent.

We have shown in this study that the combination of MRI and fluorescence imaging based on a targeted dual modal imaging agent has a potential for non-invasive tumor localization and intraoperative tumor fluorescence imaging for image-guide surgery. Contrast enhanced MR tumor imaging with a targeted agent specific to an abundantly expressed cancer biomarker can provide high resolution three dimensional visualization of tumor volume for non-invasive tumor localization and surgical planning. Intraoperative fluorescence imaging with the targeted agent can assist the operating surgeon delineate tumor boundary during the procedure. A safe and effective targeted dual modal imaging agent with high tumor specificity and binding affinity is essential for image-guided surgery. Structural optimization of the targeted dual imaging agent will be performed in the future studies to improve its tumor specificity and binding affinity.

CONCLUSIONS

A peptide targeted nanoglobular dual modal imaging agent CLT1-G2-(Gd-DOTA-MA)-Cy5 was synthesized for cancer molecular imaging with MRI and fluorescence imaging. The targeted agent resulted in significant contrast enhancement in the orthotopic prostate tumor in mice at a relatively low dose as compared to the non-targeted control KAREC-G2-(Gd-DOTA-MA)-Cy5. The targeted dual imaging agent also produced significant fluorescence signal in the tumor tissue. Structural optimization is needed to improve tumor specificity and binding affinity of the targeted dual imaging agent. The combination of MRI and fluorescence imaging based on an effective targeted dual imaging agent has a potential for accurate tumor detection and localization in image-guided cancer surgery.

ACKNOWLEDGMENTS AND DISCLOSURES

This work is supported in part by the NIH R01 CA097465. We greatly appreciate Drs. Ya Chen, Yong Chen and Wen Li for their technical assistance in MRI data acquisition.

REFERENCES

1. Gioux S, Choi HS, Frangioni JV. Image-guided surgery using invisible near-infrared light: fundamentals of clinical translation. Mol Imaging. 2010;9:237–55.
2. Mieog JS, Vahrmeijer AL, Hutteman M, van der Vorst JR, Drijfhout van Hooff M, Dijkstra J, *et al.* Novel intraoperative near-infrared fluorescence camera system for optical image-guided cancer surgery. Mol Imaging. 2010;9:223–31.
3. Ukimura O. Image-guided surgery in minimally invasive urology. Curr Opin Urol. 2010;20:136–40.
4. Bogaards A, Sterenborg HJ, Trachtenberg J, Wilson BC, Lilge L. *In vivo* quantification of fluorescent molecular markers in real-time by ratio imaging for diagnostic screening and image-guided surgery. Lasers Surg Med. 2007;39:605–13.
5. Gotoh K, Yamada T, Ishikawa O, Takahashi H, Eguchi H, Yano M, *et al.* A novel image-guided surgery of hepatocellular carcinoma by indocyanine green fluorescence imaging navigation. J Surg Oncol. 2009;100:75–9.
6. Keramidas M, Josserand V, Righini CA, Wenk C, Faure C, Coll JL. Intraoperative near-infrared image-guided surgery for peritoneal carcinomatosis in a preclinical experimental model. Br J Surg. 2010;97:737–43.
7. Frullano L, Meade TJ. Multimodal MRI contrast agents. J Biol Inorg Chem. 2007;12:939–49.
8. Olson ES, Jiang T, Aguilera TA, Nguyen QT, Ellies LG, Scadeng M, *et al.* Activatable cell penetrating peptides linked to nanoparticles as dual probes for *in vivo* fluorescence and MR imaging of proteases. Proc Natl Acad Sci U S A. 2010;107:4311–6.
9. Koyama Y, Talanov VS, Bernardo M, Hama Y, Regino CAS, Brechbiel MW, *et al.* A dendrimer-based nanosized contrast agent, dual-labeled for magnetic resonance and optical fluorescence imaging to localize the sentinel lymph node in mice. J Magn Reson Imaging. 2007;25:866–71.
10. Yiu HH, Pickard MR, Olariu CI, Williams SR, Chari DM, Rosseinsky MJ. Fe_3O_4-PEI-RITC magnetic nanoparticles with imaging and gene transfer capability: development of a tool for neural cell transplantation therapies. Pharm Res. 2012;29:1328–43.
11. Mishra A, Pfeuffer J, Mishra R, Engelmann J, Mishra AK, Ugurbil K, *et al.* A new class of Gd-based DO3A-ethylamine-derived targeted contrast agents for MR and optical imaging. Bioconjugate Chem. 2006;17:773–80.
12. Mulder WJM, Koole R, Brandwijk RJ, Storm G, Chin PTK, Strijkers GJ, *et al.* Quantum dots with a paramagnetic coating as a bimodal molecular imaging probe. Nano Lett. 2006;6:1–6.
13. Pfaff A, Schallon A, Ruhland TM, Majewski AP, Schmalz H, Freitag R, *et al.* Magnetic and fluorescent glycopolymer hybrid nanoparticles for intranuclear optical imaging. Biomacromolecules. 2011;12:3805–11.
14. Tan MQ, Wu XM, Jeong EK, Chen QJ, Lu ZR. Peptide-targeted nanoglobular Gd-DOTA monoamide conjugates for magnetic resonance cancer molecular imaging. Biomacromolecules. 2010;11:754–61.
15. Tan MQ, Wu XM, Jeong EK, Chen QJ, Parker DL, Lu ZR. An effective targeted nanoglobular manganese(II) chelate conjugate for magnetic resonance molecular imaging of tumor extracellular matrix. Mol Pharmaceut. 2010;7:936–43.
16. Pilch J, Brown DM, Komatsu M, Jarvinen TAH, Yang M, Peters D, *et al.* Peptides selected for binding to clotted plasma accumulate in tumor stroma and wounds. Proc Natl Acad Sci U S A. 2006;103:2800–4.
17. Kaneshiro TL, Jeong EK, Morrell G, Parker DL, Lu ZR. Synthesis and evaluation of globular Gd-DOTA-monoamide conjugates with precisely controlled nanosizes for magnetic resonance angiography. Biomacromolecules. 2008;9:2742–8.
18. Tan MQ, Burden-Gulley SM, Li W, Wu XM, Lindner D, Brady-Kalnay SM, *et al.* MR molecular imaging of prostate cancer with a peptide-targeted contrast agent in a mouse orthotopic prostate cancer model. Pharm Res-Dordr. 2012;29:953–60.
19. Louie AY. Multimodality imaging probes: design and challenges. Chem Rev. 2010;110:3146–95.
20. Kobayashi H, Koyama Y, Barrett T, Hama Y, Regino CAS, Shin IS, *et al.* Multimodal nanoprobes for radionuclide and five-color near-infrared optical lymphatic imaging. ACS Nano. 2007;1:258–64.
21. Kaneshiro TL, Wang X, Lu ZR. Synthesis, characterization, and gene delivery of poly-L-lySine octa(3-aminopropyl)silsesquioxane dendrimers: nanoglobular drug carriers with precisely defined molecular architectures. Mol Pharmaceut. 2007;4:759–68.
22. Kaneshiro TL, Lu ZR. Targeted intracellular codelivery of chemotherapeutics and nucleic acid with a well-defined dendrimer-based nanoglobular carrier. Biomaterials. 2009;30:5660–6.
23. Sonmez H, Suer S, Karaarslan I, Baloglu H, Kokoglu E. Tissue fibronectin levels of human prostatic cancer, as a tumor marker. Cancer Biochem Bioph. 1995;15:107–10.
24. Ye F, Wu X, Jeong EK, Jia Z, Yang T, Parker D, *et al.* A peptide targeted contrast agent specific to fibrin-fibronectin complexes for cancer molecular imaging with MRI. Bioconjug Chem. 2008;19:2300–3.
25. Yeeprae W, Kawakami S, Suzuki S, Yamashita F, Hashida M. Physicochemical and pharmacokinetic characteristics of cationic liposomes. Pharmazie. 2006;61:102–5.
26. Kurmi BD, Gajbhiye V, Kayat J, Jain NK. Lactoferrin-conjugated dendritic nanoconstructs for lung targeting of methotrexate. J Pharm Sci. 2011;100:2311–20.
27. Yu T, Hubbard D, Ray A, Ghandehari H. *In vivo* biodistribution and pharmacokinetics of silica nanoparticles as a function of geometry, porosity and surface characteristics. J Control Release. 2012;163:46–54.